



**HAL**  
open science

## Dual cells with mixed protonic-anionic conductivity for reversible SOFC/SOEC operation

Massimo Viviani, Giovanna Canu, Paola Carpanese, Antonio Barbucci, Alessandra Sanson, Elisa Mercadelli, Christiano Nicolella, Daria Vladikova, Zdravko Stoynov, Anthony Chesnaud, et al.

### ► To cite this version:

Massimo Viviani, Giovanna Canu, Paola Carpanese, Antonio Barbucci, Alessandra Sanson, et al.. Dual cells with mixed protonic-anionic conductivity for reversible SOFC/SOEC operation. Energy Procedia, 2012, Fuel Cells 2012 Science & Technology – A Grove Fuel Cell Event, 28, pp.182-189. 10.1016/j.egypro.2012.08.052 . hal-00794715

**HAL Id: hal-00794715**

**<https://minesparis-psl.hal.science/hal-00794715>**

Submitted on 20 Feb 2018

**HAL** is a multi-disciplinary open access archive for the deposit and dissemination of scientific research documents, whether they are published or not. The documents may come from teaching and research institutions in France or abroad, or from public or private research centers.

L'archive ouverte pluridisciplinaire **HAL**, est destinée au dépôt et à la diffusion de documents scientifiques de niveau recherche, publiés ou non, émanant des établissements d'enseignement et de recherche français ou étrangers, des laboratoires publics ou privés.

Fuel Cells 2012 Science & Technology – A Grove Fuel Cell Event

## Dual cells with mixed protonic-anionic conductivity for reversible SOFC/SOEC operation

Massimo Viviani<sup>\*a</sup>, Giovanna Canu<sup>a</sup>, Maria Paola Carpanese<sup>a</sup>,  
Antonio Barbucci<sup>a,b</sup>, Alessandra Sanson<sup>c</sup>, Elisa Mercadelli<sup>c</sup>, Cristiano Nicoletta<sup>d</sup>,  
Daria Vladikova<sup>e</sup>, Zdravko Stoynov<sup>e</sup>, Anthony Chesnaud<sup>f</sup>, Alain Thorel<sup>f</sup>,  
Zeynep Ilhan<sup>g</sup>, Sayed-Asif Ansar<sup>g</sup>

<sup>a</sup>Institute for Energetics and Interphases (CNR-IENI), Via De Marini 6, 16149 Genova, Italy

<sup>b</sup>Dept. of Process and Chemical Engineering (DICheP), University of Genova, P. le Kennedy 1, 16129 Genova, Italy

<sup>c</sup>Institute of Science and Technology of Ceramics (CNR-ISTEC), Via Granarolo 64, 48018 Faenza, Italy

<sup>d</sup>Dept. of Chemical Engineering (DICCISM), University of Genova, P. le Kennedy 1, 16129 Genova, Italy

<sup>e</sup>Institute of Electrochemistry and Energy Systems, Bulgarian Academy of Sciences, 10 Acad. G. Bonchev St., 1113 Sofia, Bulgaria

<sup>f</sup>Centre des Matériaux, UMR CNRS 7633, Mines-ParisTech, BP 87, F-91003 Evry Cedex, France

<sup>g</sup>Institute of Technical Thermodynamics, German Aerospace Center (DLR-ITT), Pfaffenwaldring 38–40, D-70569 Stuttgart, Germany

### Abstract

The dual cell concept is a novel design for solid oxide fuel cells operating at intermediate temperature. The cell comprises a series of five layers with different compositions, alternating two dense electrolytes and three porous layers, i.e. the outer electrodes and a central membrane. The dual cell concept makes it possible to separate the compartment for water formation from both fuel and oxidant chambers. Such a three-chamber configuration gives many advantages related to fuel dilution, materials corrosion, and reversibility between fuel cell and electrolyser operational modes (SOFC/SOEC) at high temperature. Dual conductivity (protonic/anionic) can be achieved by joining two dense  $\text{BaCe}_{0.85}\text{Y}_{0.15}\text{O}_{3-\delta}$  (BCY) and  $\text{Ce}_{0.85}\text{Y}_{0.15}\text{O}_{2-\delta}$  (YDC) electrolytes through a porous ceramic central membrane made up of both materials. Complete anode-supported dual cells have been fabricated by a combination of pressing, casting, printing, wet spraying, and plasma spraying techniques. Electrochemical tests carried out by impedance spectroscopy showed the feasibility of the concept and successful reversible operation of the dual cell. The fabrication route, the microstructural and electrochemical testing results are reported in this work, and partially compared to simulated results from an electrochemical model developed describing the dual cell concept.

© 2012 Published by Elsevier Ltd. Selection and/or peer-review under responsibility of the Grove Steering Committee.

**Keywords:** Solid oxide fuel cells; Proton conductors; Dual membrane; Plasma spraying

\* Corresponding author. Tel: +39-010-6475-705; fax: +39-010-6475-700.

E-mail address: [m.viviani@ge.ieni.cnr.it](mailto:m.viviani@ge.ieni.cnr.it)

**1. Introduction**

Solid oxide fuel cell (SOFC) technology is receiving increasing scientific and industrial interest for a number of stationary and portable applications, like combined heat and power (CHP) systems and auxiliary power units (APUs) [1]. The same technology is being considered for the reverse operation, i.e. the production of H<sub>2</sub> gas by high-temperature electrolysis (solid oxide electrolysis cell, SOEC), especially combined with renewable sources or nuclear plants [2].

The main limitations to SOFC/SOEC systems are represented by stack degradation over long-term operation, and resistance to thermal and redox cycling, which could be mitigated by lowering the operating temperature, e.g. by adopting proton conducting electrolytes [3]. The presence of water at either cathode or anode is also unfavourable because of negative effects on fuel utilisation, electrode stability, and metallic interconnect durability [4].

The architecture of the Dual Membrane Cell (DM-Cell) combines all the advantages of protonic SOFCs without the drawbacks associated with the presence of water at the electrodes. In such a three-chamber cell water is produced in a mixed H<sup>+</sup> and O<sup>2-</sup> conducting membrane, which also allows easy reverse operation as an electrolysis cell without any adjustment to the composition of feed gases.

Fig. 1 shows the schematic of a DM-Cell principle. When operating in SOFC mode, H<sup>+</sup> and O<sup>2-</sup> ions are formed at the anode and cathode, respectively, migrate through the protonic and anionic electrolyte towards the dual membrane placed in the middle of the cell, and there recombine to form water vapour. The SOEC operating mode is obtained by just reversing the polarisation and feeding pure water vapour in the Dual Membrane compartment. The formation of H<sub>2</sub>O in a separate compartment should reduce corrosion of interconnects and remove the need for drying in the case of fuel gas recirculation.

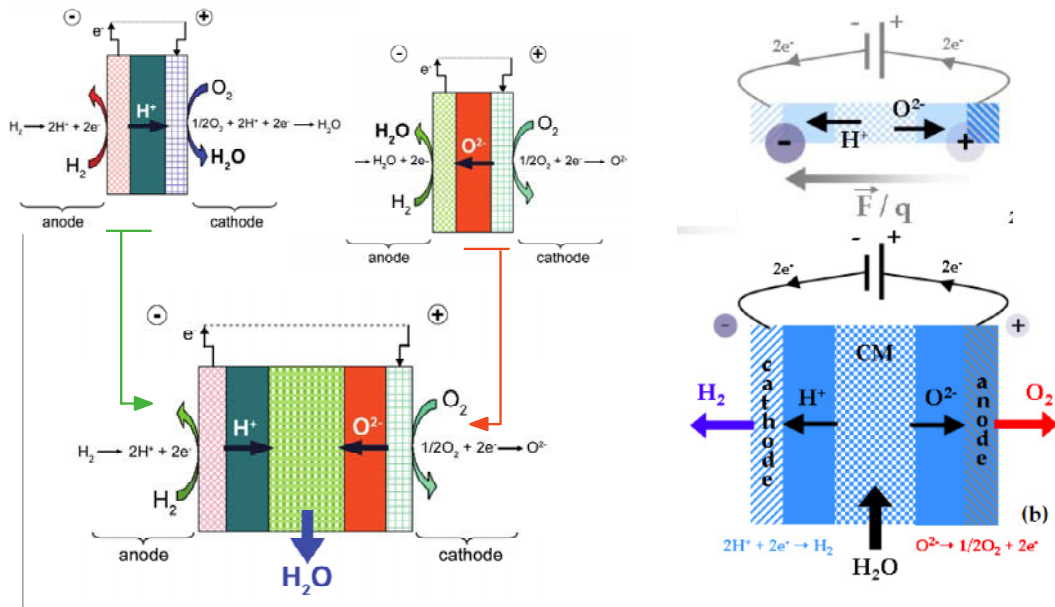


Fig. 1. (a) The DM-Cell principle in SOFC mode. (b) The DM-Cell principle in SOEC mode.

## 2. Proof of the concept and modelling

The concept of a DM-Cell was proven in a series of dedicated experiments focusing on four different criteria: (1) establishment of a stable OCV, (2) measurement of electric current under load (i-V curve), (3) detection of water formation by electrochemical impedance spectroscopy (EIS), and (4) correlation between polarisation and water production in the DM compartment [5]. Fig. 2 clearly shows the humidity change in the  $N_2$  gas streaming through the DM compartment, across polarisation switching cycles in a complete DM-Cell (criterion 4).

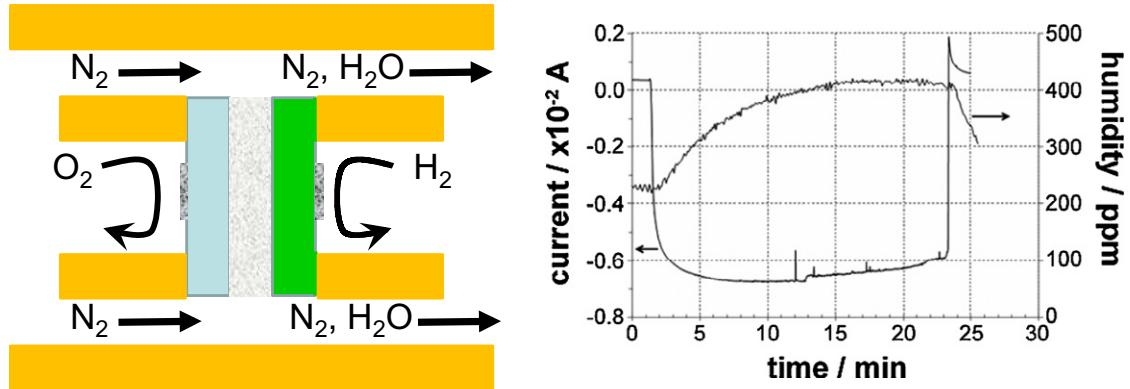


Fig. 2. (a) Schematic of the three-chamber tester used to make the proof of the concept. (b) Electric current flowing through the cell and moisture concentration in the DM compartment vs. time. (Reprinted from [5])

The operation of the DM fuel cell was simulated by means of a microkinetic mathematical model which takes into account charge transfer, mass transfer, and electrochemical reactions in the cell, and enables the prediction of the steady-state and dynamic response of the DM-Cell under varying operating conditions [6].

The model was validated on polarisation data experiments carried out for the proof of concept (Fig. 3a). The effect of the DM thickness on the cell performance was investigated. A thick layer hosts a large number of active reaction sites, with reduced current flux per single contact point. As a consequence, thick layers show low activation resistance, but they may be affected by high ohmic losses. Moreover, thin layers have low ohmic losses, but due to the reduced number of active reaction sites, they are characterised by high activation losses. As a result, for any given selection of materials, morphology (particle size  $d_p = 0.4 \mu\text{m}$ , volume fraction of pore  $\varepsilon = 0.25$ ) and operating conditions (i.e. temperature), an optimum thickness can be identified (Fig. 3), with balanced ohmic and activation resistances to provide minimum energy losses. The calculated polarisation curve reveals that  $120 \mu\text{m}$  corresponds to the thickness leading to the best cell performance, which gives comfortable latitude for shaping (Fig. 3b).

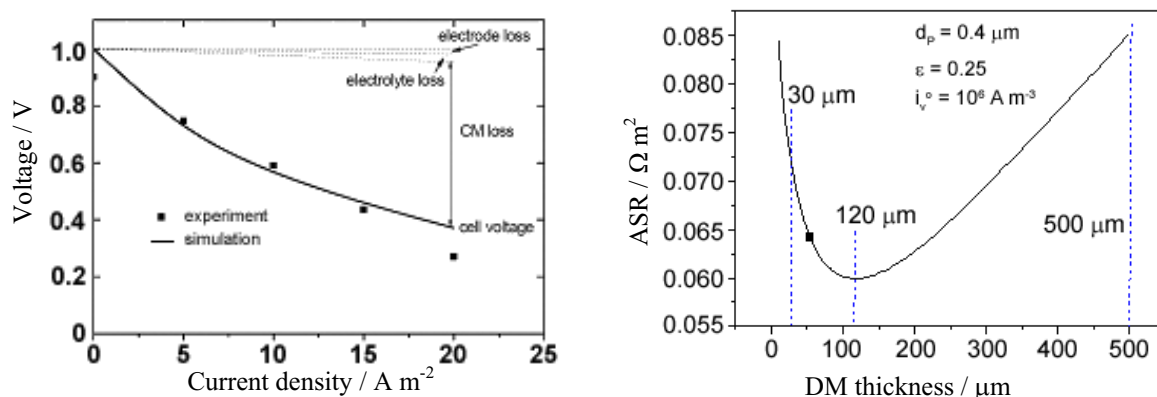


Fig. 3. (a) Model validation by comparison with the polarisation curve of a DM-Cell. (b) Calculated area specific resistance (ASR) vs. thickness of dual membrane. The kinetic parameter  $i_v^0$  was estimated by fitting with experimental data.

### 3. Experimental

The feasibility and the potential performance of the DM-Cell have been explored by applying easily scaled-up fabrication processes, like tape casting and spraying.  $\text{BaCe}_{0.85}\text{Y}_{0.15}\text{O}_{3-\delta}$  (BCY) powders were employed for the fabrication of protonic electrolyte and cermet anode layers,  $\text{Ce}_{0.85}\text{Y}_{0.15}\text{O}_{2-\delta}$  (YDC) powders were adopted for the anionic electrolyte. A mixture (50 vol%) was used to realise DM layers. The average particle size for both compositions was about 200 nm, and for plasma spraying an additional granulation step was carried out in order to form larger aggregates. Cathodic layers were made of  $\text{La}_{0.6}\text{Sr}_{0.4}\text{Co}_{0.2}\text{Fe}_{0.8}\text{O}_{3-\delta}$  (LSCF). In the case of tape cast cells, all layers of the DM-Cell were made of BCY, in order to take advantage of the dual (anionic-protonic) conductivity of this perovskite structure [7] and simplify the multilayer structure fabrication.

#### 3.1. Sprayed cell

All five functional layers of a DM-Cell were developed separately by applying thermal spraying technologies. A 48 mm diameter cell with a total functional layer thickness of 180 μm was successfully fabricated. In Fig. 4 a cross-sectional view of the plasma sprayed dual cell deposited on a 1000 μm thick porous metallic substrate can be seen after 250 h of operation at 600°C and 700°C. A 35 μm thick anode layer of BCY and Ni cermet was deposited onto the substrate, and exhibited sufficient porosity after being reduced at high temperature. This was followed by a relatively dense 35 μm thick BCY electrolyte possessing substantially globular and closed porosity, which ensured an acceptable gas leakage rate. A 45 μm thick porous composite DM was deposited on the protonic electrolyte, exhibiting a very good adherence along the radial axis. The second electrolyte YDC was deposited with 50 μm thickness and a relatively higher rate of microcracks, and finally an 10–15 μm LSCF paste was applied which was annealed in situ.

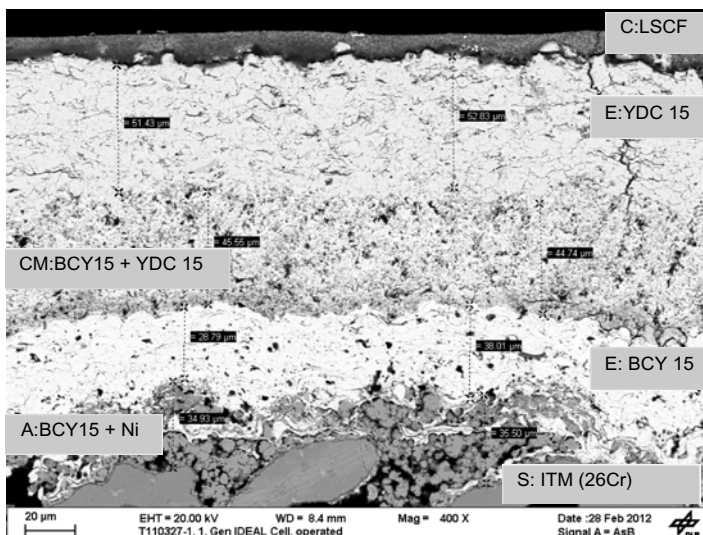


Fig. 4. Cross-section SEM image of plasma sprayed DM-Cell. C: cathode, E: electrolyte, CM: dual membrane, A: anode, and S: metallic substrate.

### 3.2. Tape cast cells

Trilayers of BCY/BCY-porous/BCY were fabricated by tape casting, lamination and successive co-firing. Sintering at 1400°C for 4 h gave almost flat, crack-free, 570 μm thick multilayers. Perfect adhesion of the three laminated layers was also obtained. The central 40 μm thick porous zone is sandwiched between two properly dense layers, as clearly shown in Fig. 5.

Rice starch (RS, Fluka), with average particle size of 6 μm was used as the sacrificial pore-forming agent. The slurries were prepared by adding to the starting ceramic powders the desired amounts of solvent, deflocculant, binder, and plasticiser. The ball milled suspension was de-aerated under vacuum and cast on a moving Mylar carrier ( $v = 6$  mm/s), to obtain, after solvent evaporation, green tapes with the desired thickness.

A uniaxial warm press was used to laminate the green tape layers. The layers with 40 mm diameter were stacked between two polished parallel steel plates, and heated for 15 min at 55°C. During the thermal treatment a constant loading of 7.3 MPa was maintained.

Samples for electrochemical characterisation were electroded with a Pt layer on both sides, realised by screen printing.

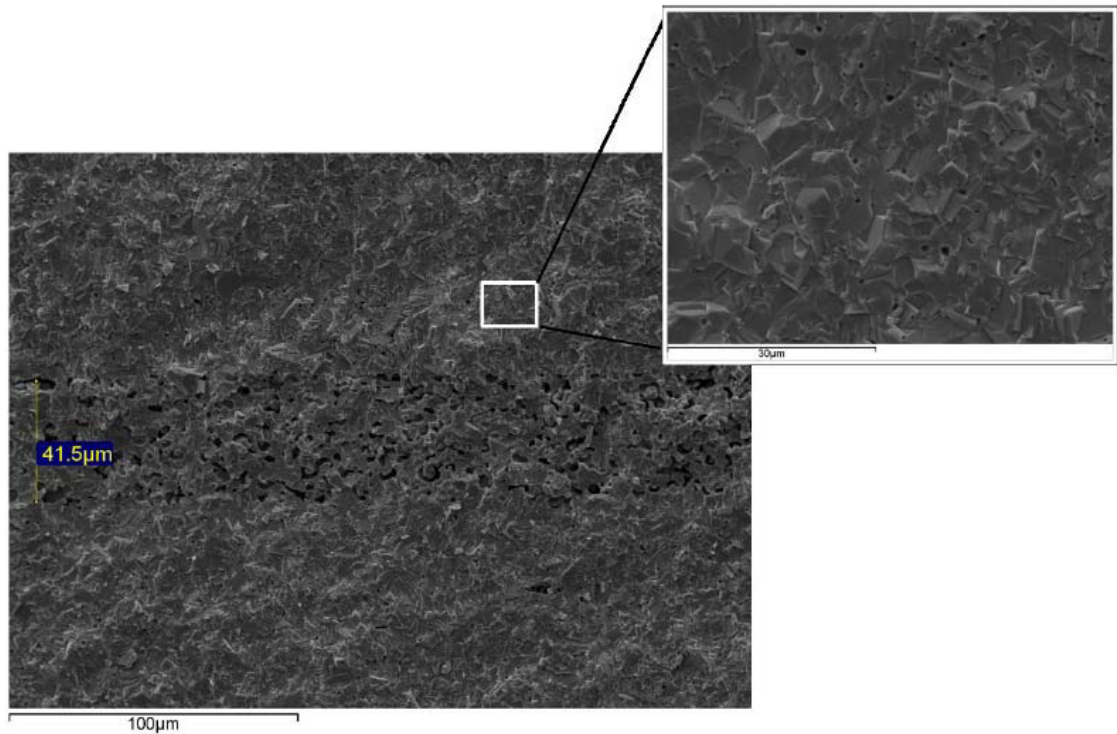


Fig. 5. Cross-section SEM image of a tape cast-laminated DM-Cell. Inset shows the density of the electrolyte layers.

#### 4. Results and discussion

A metal supported dual cell was tested in a two-chamber setup for 250 h with 50% H<sub>2</sub>-50% N<sub>2</sub> and air at the anode and cathode chamber, respectively. The long-term measurement was interrupted to record several polarisation curves at different temperature and gas supply combinations (Fig. 6a).

In Fig. 6b the maximum power density achieved by the dual cell is presented as 132 mW/cm<sup>2</sup>, 75 mW/cm<sup>2</sup>, and 39 mW/cm<sup>2</sup> for 800, 700, and 600°C, respectively for hydrogen/oxygen supply. The results show satisfactory gas tightness of the electrolytes, and notable stability in the performance. When compared to intermediate-temperature SOFCs (IT-SOFCs) and protonic ceramic fuel cells (PCFCs) prepared by the same fabrication technology, the DM-Cell resulted in lower performance (by a factor of between 3 and 10), possibly due to the non-optimised microstructure of the porous DM, the most challenging structure for plasma spraying.

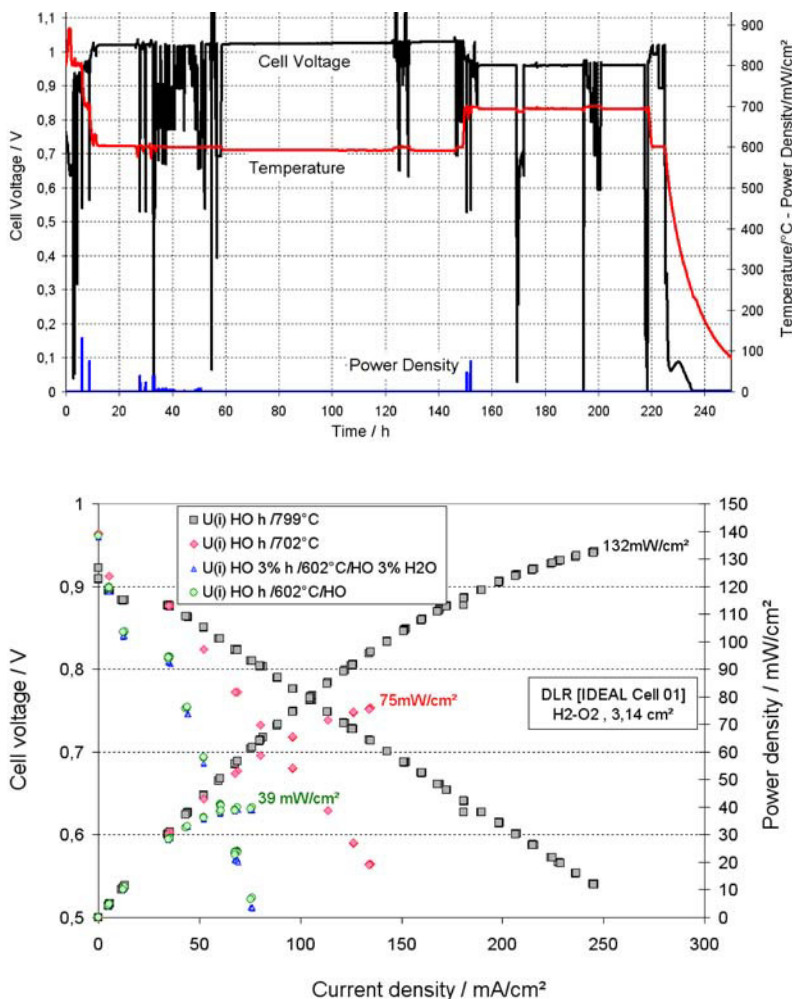


Fig. 6. (a) Life cycle diagram of the plasma sprayed DM-Cell; cell voltage plotted as a function of the time and temperature at a constant gas flow (dry hydrogen and air). (b) Current density/voltage and power density curves of plasma sprayed DM-Cell as a function of the temperature at a constant gas flow (dry hydrogen and oxygen and 3% wet hydrogen and oxygen).

Monolithic cells fabricated by tape casting were tested in both SOFC and SOEC mode in a two-chamber setup at different temperatures in the range 600–800°C. In order to highlight the special feature of the DM, a conditioning step was carried out by first polarising the cell in SOFC mode under wet H<sub>2</sub>–air feeding for 20 min. This conditioning was then followed by SOEC polarisation with N<sub>2</sub>–N<sub>2</sub> (dry or wet–3 at%) feeding. Results for 600°C are reported in Fig. 7, and compared to the same experiment without conditioning, i.e. H<sub>2</sub>–air feeding at OCV. A lower resistance was always found after conditioning, with little effect of additional steam injected during polarisation. This result suggests that enhanced water splitting takes place in the DM-Cell due to some form of accumulation of OH<sup>-</sup> ions, possibly as an adsorbed film at the pores surface in the DM, and confirms the feasibility of a reversible device with the DM-Cell architecture.

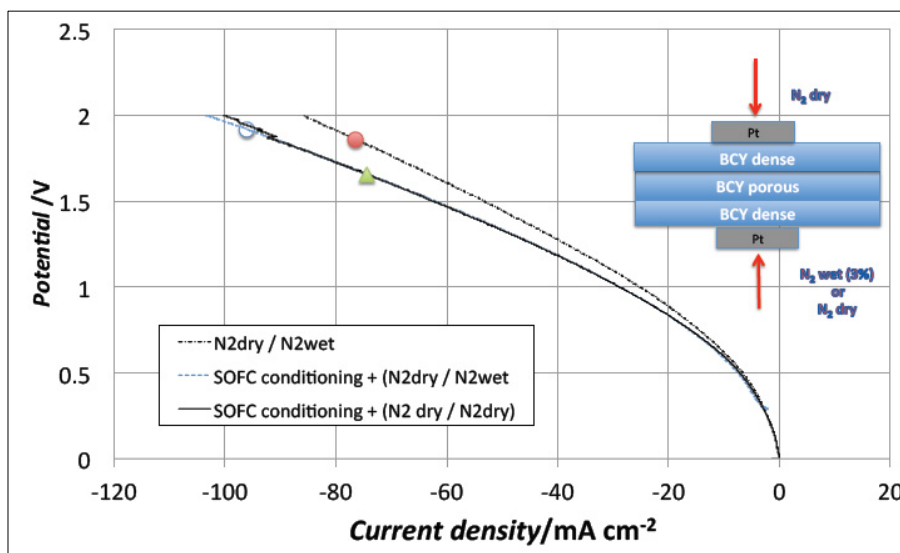


Fig. 7. Polarisation curves in SOEC mode at 600°C. Solid circle: no conditioning and wet feeding, empty circle: conditioning and wet feeding, triangle: conditioning and dry feeding.

## 5. Conclusions

The DM-Cell is an innovative SOFC concept combining protonic and anionic conductivity, and providing an independent compartment for water formation. Thanks to the IDEAL-Cell project this technology has almost reached protonic ceramic fuel cell standards after only four years of development, and is suitable for fabrication with different industrial processes like plasma spraying and tape casting.

The DM-Cell architecture is particularly favourable for reversible SOFC/SOEC operation.

## Acknowledgments

Powders were fabricated and supplied by Marion Technologies (Verniole, France). The research leading to these results has received funding from the European Community's Seventh Framework Programme under grant agreement no. 213389, Project IDEAL-Cell (2008–2011).

## References

1. R. Rivera-Tinoco, K. Schoots, B. van der Zwaan, Learning curves for solid oxide fuel cells, *Energy Conversion and Management* 2012; **57**: 86–96.
2. S.D. Ebbesen, J. Høgh, K.A. Nielsen, J.U. Nielsen, M. Mogensen, Durable SOC stacks for production of hydrogen and synthesis gas by high temperature electrolysis, *Int. J. Hydrogen Energy* 2011; **36**: 7363–7373.
3. P. Holtappels, U. Vogt, T. Graule, Ceramic materials for advanced solid oxide fuel cells, *Advanced Engineering Materials* 2005; **7**: 292–302.
4. P. Piccardo, P. Gannon, S. Chevalier, M. Viviani, A. Barbucci, G. Caboche, ASR evaluation of different kinds of coatings on a ferritic stainless steel as SOFC interconnects, *Surface and Coatings Technology* 2007; **202**: 1221–1225.
5. D. Vladikova, Impedance spectroscopy studies of dual membrane fuel cell, *Electrochimica Acta* 2011; **56**: 7955–7962.
6. A. Bertei, C. Nicolella, F. Delloro, W.G. Bessler, N. Bundschuh, A. Thorel, Mathematical modeling and simulation for optimization of IDEAL-Cell performance. Solid Oxide Fuel Cells 12 (SOFC-XII), *ECS Trans.* 2011; **35**(1): 883.
7. S. Ricote, N. Bonanos, G. Caboche, Water vapour solubility and conductivity study of the proton conductor  $\text{BaCe}_{0.9-x}\text{Zr}_x\text{Y}_{0.1}\text{O}_{3-\delta}$ , *Solid State Ionics* 2009; **180**: 990–997.